Guanylate-binding proteins promote activation of the AIM2 inflammasome during infection with Francisella novicida

Etienne Meunier, Pierre Wallet, Roland Dreier, Stéphanie Costanzo, Leonie Anton, Sebastian Rühl, Sebastien Dussurgey, Mathias Dick, Anne Kistner, Mélanie Rigard, et al.

Nat Immunol. Author manuscript; available in PMC 2015 November 01.

Published in final edited form as:
Nat Immunol. 2015 May ; 16(5): 476–484. doi:10.1038/ni.3119.

Guanylate-binding proteins promote AIM2 inflammasome activation during *Francisella novicida* infection by inducing cytosolic bacteriolysis and DNA release

Etienne Meunier[#1], **Pierre Wallet**[#2], **Roland F. Dreier**[1], **Stéphanie Costanzo**[2], **Leonie Anton**[1], **Sebastian Rühl**[1], **Sébastien Dussurgey**[3], **Mathias S. Dick**[1], **Anne Kistner**[1], **Mélanie Rigard**[2], **Daniel Degrandi**[4], **Klaus Pfeffer**[4], **Masahiro Yamamoto**[5], **Thomas Henry**[2,*], and **Petr Broz**[1,*]

[1]Focal Area Infection Biology, Biozentrum, University of Basel, Basel, Switzerland [2]CIRI, Inserm U1111, CNRS UMR 5308, Université Claude Bernard Lyon-1, Ecole Normale Supérieure, Lyon, France. [3]SFR Biosciences, UMS344/US8, Inserm, CNRS, Université Claude Bernard Lyon-1, Ecole Normale Supérieure, Lyon, France. [4]Institute of Medical Microbiology and Hospital Hygiene, Heinrich-Heine-University Duesseldorf, Duesseldorf 40225, Germany [5]Department of Microbiology and Immunology, Osaka University, Yamadaoka, Suita, Osaka 565-0871, Japan

[#] These authors contributed equally to this work.

Abstract

The AIM2 inflammasome detects double-stranded DNA in the cytosol and induces caspase-1-dependent pyroptosis as well as release of the inflammatory cytokines IL-1β and IL-18. AIM2 is critical for host defense against DNA viruses and bacteria that replicate in the cytosol, such as *Francisella novicida.* AIM2 activation by *F. novicida* requires bacteriolysis, yet whether this process is accidental or a host-driven immune mechanism remained unclear. Using siRNA screening for nearly 500 interferon-stimulated genes, we identified guanylate-binding proteins GBP2 and GBP5 as key AIM2 activators during *F. novicida* infection. Their prominent role was validated *in vitro* and in a mouse model of tularemia. Mechanistically, these two GBPs target cytosolic *F. novicida* and promote bacteriolysis. Thus, besides their role in host defense against vacuolar pathogens, GBPs also facilitate the presentation of ligands by directly attacking cytosolic bacteria.

The innate immune system detects invading pathogens through membrane-bound and cytosolic pattern recognition receptors (PRRs), which recognize microbial- and damage-associated molecular patterns (MAMPs and DAMPs) and induce conserved signaling

[*]Co-corresponding authors: Petr Broz, Ph.D. Assistant Professor Focal Area Infection Biology Biozentrum, University of Basel Klingelbergstrasse 50/70 CH-4056 Basel / Switzerland petr.broz@unibas.ch phone: +41 61 267 23 42 fax: +41 61 267 21 18 or thomas.henry@inserm.fr (TH) .

AUTHOR CONTRIBUTIONS E.M, P.W., T.H. and P.B. conceived of the research. T.H. and P.B. wrote the manuscript; E.M., P.W., R.F.D., L.A., S.C., S.R., M.S.D., S.D., A.K., M.R., T.H. and P.B. performed experiments; D.D., K.P. and M.Y. provided reagents.

COMPETING FINANCIAL INTERESTS The authors declare no competing financial interests.

Europe PMC Funders Author Manuscripts

pathways. Nucleic acids and their derivatives are detected by RIG-I-like receptors, cGAS, DAI and RNA polymerases, resulting in type-I-interferon (type-I-IFN) induction via STING and TBK1[1-3]. Cytosolic microbial and host DNA also induces inflammasome formation through the PYHIN family member AIM2 (absent in melanoma 2)[4-7]. AIM2 binds double-stranded DNA through its HIN-200 domain[8] and recruits the inflammasome adaptor protein ASC. ASC rapidly oligomerizes to form a macromolecular inflammasome complex known as an ASC speck that activates caspase-1. Active caspase-1 promotes the maturation and release of pro-inflammatory cytokines interleukin (IL)-1β and IL-18. In addition it induces pyroptosis, a lytic form of cell death that restricts pathogen replication. The AIM2 inflammasome mediates recognition of DNA viruses as well as a number of Gram-negative and Gram-positive cytosolic bacteria like *Listeria monocytogenes*, *Legionella pneumophila*, *Mycobacterium* spp. and *Francisella tularensis* subspecies *novicida* (hereafter referred to as *F. novicida*)[8-14]. Importantly, several studies have shown that AIM2 activation by these bacteria requires bacteriolysis and the subsequent release of bacterial chromosomal DNA into the cytosol[10, 12, 15]. Yet, whether bacteriolysis is accidental or an active, host-directed mechanism is unclear.

AIM2 activation by transfection of synthetic DNA or during DNA virus infection is independent of Toll-like receptor (TLR)- or interferon-signaling[9, 13, 16]. In stark contrast, AIM2 activation during *F. novicida* infection requires the production of type-I-IFNs, which are induced as a result of the recognition of a yet undefined *F. novicida*-derived nucleic ligand in the cytosol [9, 10, 17, 18, 19, 20]. Consistent with this AIM2 inflammasome activation in *F. novicida*-infected cells requires signaling through STING and the transcription factor IRF3[9, 10, 17]. It was speculated that IFN-signaling is necessary to increase cellular AIM2 in order to detect *F. novicida* DNA[9], yet IFN-mediated AIM2 induction is contested and even low amounts of transfected DNA efficiently trigger AIM2 activation in an IFN-independent manner[9]. Therefore it is likely that one or several IFN-inducible factors are required for efficient activation of AIM2 during bacterial infections.

Type-I- and Type-II-IFNs are potent cytokines that exert anti-microbial effects through the induction of a broad transcriptional program involving ~2000 genes, so-called IFN-stimulated genes (ISGs), many of which remain uncharacterized. Prominent among these ISGs are several families of interferon-inducible GTPases, such as the 47-kD immunity-related GTPases (IRGs) and the 65- to 73-kD guanylate-binding proteins (GBPs)[21, 22]. GBPs are conserved among vertebrates, with 11 GBPs in mice and 7 in humans, and exhibit anti-microbial effects against intracellular bacteria and protozoa[23]. GBP1 and GBP7 restrict *Mycobacterium bovis* BCG and *Listeria monocytogenes* by recruiting antimicrobial effectors to the pathogen-containing vacuole (PCV)[24]. Several GBPs are recruited onto the *Toxoplasma* parasitophorous vacuole[25] and most are also required for restricting *T. gondii* replication[23, 26-28]. In addition, GBPs on murine chromosome 3 promote innate immune recognition of the vacuolar, Gram-negative bacterium *Salmonella typhimurium* by destabilizing its PCV, leading to the egress of bacteria into the cytosol and subsequent detection of lipopolysaccharide (LPS) by the caspase-11 inflammasome[29]. In this study we found that GBPs on murine chromosome 3 were a key factor for AIM2 activation during *F. novicida* infection. In particular GBP2 and GBP5 controlled AIM2 activation by targeting

cytosolic *F. novicida* and inducing their lysis by a yet uncharacterized mechanism. We demonstrate that GBP-deficient mice are unable to control *F. novicida* infection *in vivo*. Altogether our data reveal a function for GBPs during microbial infections, in that GBPs promote bacteriolysis in the cytosol and the exposure of bacterial DNA to cytosolic innate immune sensors.

RESULTS

AIM2 activation during *F. novicida* infection requires IFNs

F. novicida is a facultative intracellular Gram-negative bacterium that avoids phagosomal degradation in phagocytes by escaping into the cytosol, a process that requires the *Francisella* Pathogenicity Island (FPI). Following phagosomal escape, *F. novicida* replicates in the cytosol, but also triggers AIM2-dependent caspase-1 activation[10, 13]. Infection of murine bone-marrow derived macrophages (BMDMs) with wild-type *F. novicida* resulted in cell death (pyroptosis, measured by lactate dehydrogenase (LDH) release) and IL-1β release dependent on AIM2, ASC and caspase-1, while a ΔFPI mutant did not activate the inflammasome (Fig. 1a). The signaling molecule STING (gene name *Tmem173* but hereafter referred to as *Sting*) is linked to AIM2 activation during *F. novicida* infection[10, 12]. *Sting*-deficient (Goldenticket ENU *Sting* mutant, hereafter $Sting^{Gt/Gt}$) macrophages were strongly attenuated in their ability to induce type-I-IFN expression and AIM2 inflammasome activation upon *F. novicida* infection (Fig. 1b, Supplementary Fig. 1a)[5]. Consistent with an important role for type-I-IFN in AIM2 inflammasome activation[17, 19], macrophages from mice deficient in *Ifnar1* (interferon alpha and beta receptor 1) or *Stat1* (signal transducer and activator of transcription 1) displayed a significant reduction in pyroptosis and IL-1β release when infected with *F. novicida* (Fig. 1c). To further confirm that AIM2 activation during *F. novicida* infection depended on type-I-IFN signaling, we tested if exogenous interferons could rescue inflammasome activation in *Sting*-deficient BMDMs. As expected, IFN-β restored cell death and cytokine release in $Sting^{Gt/Gt}$ BMDMs (Fig. 1d). IFN-γ addition restored cell death and cytokine release in both $Sting^{Gt/Gt}$ and $Ifnar1^{-/-}$ BMDMs (Fig. 1d), indicating a requirement for a general IFN signature.

Induction of *Aim2* mRNA could account for the strong dependency on type-I-IFN (STAT-1) signaling during *F. novicida* infection[10]. However, activation of the AIM2 inflammasome by DNA transfection or infection with DNA viruses is independent of interferon-signaling[9, 13, 16]. In accordance with these reports, induction of cell death by transfection of 1 μg/ml poly (deoxyadenylic-deoxythymidylic) acid (poly(dA:dT)) required AIM2, but was completely independent of STING and STAT-1 (Fig. 1e). Transfection of large amounts of DNA could overload the system and render it independent of IFN signaling. To rule out this possibility, we titrated down the transfected DNA. AIM2 activation remained interferon-independent even upon transfection of small quantities of DNA (Fig. 1e). These results indicated that basal AIM2 is sufficient to initiate inflammasome activation[9, 13]. Indeed only weak induction of *Aim2* mRNA was observed following *F. novicida* infection (Supplementary Fig. 1b).

Finally, we confirmed that *F. novicida* genomic DNA was equally stimulatory as synthetic DNA by transfecting increasing amounts of both into macrophages (Fig. 1f). Both types of

DNA triggered comparable cell death and IL-1β release, thus excluding the possibility that *F. novicida* DNA had properties that allowed it to evade AIM2 recognition. Taken together, these results indicated that one or several IFN-β or IFN-γ-inducible genes were required to activate AIM2 specifically during bacterial infections.

RNAi screening for AIM2 activators identifies GBP family

To identify ISGs involved in *F. novicida*-mediated AIM2 inflammasome activation, we performed RNA interference screening in BMDMs. We selected 443 genes based on at least a two fold higher expression in wild-type compared to *Ifnar1*$^{-/-}$-infected macrophages and 40 additional genes based on other reports[9, 10, 17, 18] (Supplementary Table 1). 48 hours post-siRNA transfection, macrophages were infected with *F. novicida* and inflammasome activation was monitored by determining IL-1β release and propidium iodide (PI) incorporation as a measure of cell death (Fig. 2a). Knock-down of most of the 483 genes did not significantly affect IL-1β release or cell death. In striking contrast, *Gbp2* and *Gbp5* knock-down strongly reduced *F. novicida*-mediated IL-1β release and macrophage death (Fig. 2a, black arrows), while knock-down of other *Gbp* genes showed no comparable effect (Fig. 2a, marked in red) *Gbp2* and *Gbp5* were the most expressed genes of the GBP family in macrophages and were strongly and specifically induced upon wild-type *F. novicida* infection in a STING- and IFNAR-dependent manner, but independently of *Tlr2* and *Myd88* (Fig. 2b, Supplementary Fig. 1c-e). The efficiency of siRNA-mediated knockdown of *Gbp* genes expressed during *F. novicida* infection was confirmed by RT-PCR (Supplementary Fig. 2a). We next validated the screening results by knocking down all 11 murine *Gbp* genes individually and measuring cell death and IL-1β release (Fig. 2c). Knock-down of *Gbp2* and *Gbp5* specifically decreased *F. novicida*-mediated IL-1β release and cell death as assessed by two different techniques (Fig. 2c and Supplementary Fig. 2b). In conclusion, our screening approach identified GBP2 and GBP5 as two possible ISGs that control AIM2 activation during *F. novicida* infection.

GBPs on chromosome 3 are required for AIM2 activation

To confirm our screening data, we infected naive or primed macrophages from wild-type, *Casp-1*$^{-/-}$*Casp-11*$^{-/-}$ double knockouts or *Gbp*^{chr3}-deleted mice, which lack GBP1, GBP2, GBP3, GBP5 and GBP7 on murine chromosome 3 [23], with *F. novicida*. Consistent with defective AIM2 inflammasome activation, *Gbp*^{chr3}-deleted BMDMs displayed a significant reduction in cell death and cytokine release, and had reduced processed caspase-1 p20, even though procaspase-1, ASC and AIM2 protein expression were comparable to wild-type cells (Fig. 3a-b, Supplementary Fig. 3a). Measuring propidium iodide incorporation following infection in real time showed that *Gbp*^{chr3}-deleted BMDMs died with delayed kinetics as compared to wild-type cells and similarly to *Ifnar1*$^{-/-}$ BMDMs (Supplementary Fig. 3b). To test if GBPs on chromosome 3 were directly involved in AIM2 activation, we engaged AIM2 by transfecting unprimed wild-type and *Gbp*^{chr3}-deleted macrophages with synthetic DNA (Fig. 3c). Cytosolic DNA triggered LDH release to a similar extent in both wild-type and *Gbp*^{chr3}-deleted cells, even when the amount of transfected DNA was titrated down (Fig. 3c). Wild-type, *Gbp*^{chr3}-deleted and *Ifnar1*$^{-/-}$ also responded comparably to transfection of purified *F. novicida* genomic DNA (Fig. 3d). Thus, GBPs were not required

in the context of DNA transfection suggesting that they functioned upstream of AIM2-mediated DNA detection.

GBP2 and GBP5 direct parallel pathways of AIM2 activation

Since our screening data suggested that mainly GBP2 and GBP5 are required for AIM2 activation (Fig. 2a), we infected BMDMs from wild-type, *Casp-1*$^{-/-}$*Casp-11*$^{-/-}$, *Gbp*^{chr3}-deleted, *Gbp2*$^{-/-}$ or *Gbp5*$^{-/-}$ mice with *F. novicida* and measured AIM2 inflammasome activation. *Gbp2*$^{-/-}$ BMDMs displayed reduced cell death and cytokine release compared with wild-type BMDMs (Fig. 4a-b). Similarly, *Gbp5*$^{-/-}$ BMDMs also displayed attenuated inflammasome activation when infected with *F. novicida* (Fig. 4a-b). *Gbp2*- or *Gbp5*-deficiency did not affect cell death in response to DNA transfection (Fig. 4c), even when using very low amounts of DNA. To determine if expression of GBP2 or GBP5 could restore AIM2 inflammasome activation in *Ifnar1*$^{-/-}$ cells, we infected macrophages retrovirally-transduced with constructs expressing GBP2 or GBP5, or an empty vector control (Supplementary Fig. 4a-c). Ectopic expression was not able to complement the deficiency in inflammasome activation, suggesting that other ISGs might be required for GBP2 and GBP5 function, in line with data showing that GBPs are only active and correctly targeted in the context of the IFN response[25].

Single deficiencies in *Gbp2* or *Gbp5* did not reduce AIM2 activation during *F. novicida* infection as strongly as *Gbp*^{chr3}-deficiency (Fig. 4a-b), suggesting that these two GBPs promote AIM2 activation through independent pathways. To test whether GBP2 and GBP5 acted sequentially or in parallel, we knocked down *Gbp2* expression in wild-type, *Gbp2*$^{-/-}$ and *Gbp5*$^{-/-}$ BMDMs and measured inflammasome activation after *F. novicida* infection (Fig. 4d, Supplementary Fig. 4d). *Gbp2*-knock-down reduced cell death and IL-1β release in wild-type BMDMs but not in *Gbp2*-deficient cells (Fig. 4d). *Gbp2* siRNA also significantly reduced inflammasome activation in *Gbp5*$^{-/-}$ BMDMs, demonstrating that in *Gbp5*-deficient cells GBP2 was still active and could promote AIM2 activation. Consistent with this, *Gbp5*-knock-down reduced inflammasome activation in both wild-type and *Gbp2*$^{-/-}$ BMDMs (Fig. 4d). In conclusion, our data suggested that IFN-inducible GTPases GBP2 and GBP5 control non-redundant, parallel pathways that promote AIM2 activation during *F. novicida* infection.

Phagosomal escape of *F. novicida* is GBP independent

Since cytosolic localization of *F. novicida* is required for AIM2 activation and since GBPs promote the destabilization of phagosomes and/or pathogen-containing vacuoles of protozoan parasites or bacteria[23, 27, 29], we speculated that GBPs might facilitate the phagosomal escape of *F. novicida*. A phagosome protection assay[29, 30] based on selective permeabilization of the plasma membrane with digitonin was used to assay phagosomal escape of *F. novicida* (Fig. 5a). As reported previously[30], we observed that 90-95% of wild-type *F. novicida* escaped from the phagosome within a few hours post infection, but this percentage was comparable between wild-type and *Gbp*^{chr3}-deleted BMDMs at different timepoints post infection (Fig. 5a). In contrast, ΔFPI mutant bacteria remained in the phagosome (data not shown).

F. novicida is naturally resistant to β-lactam antibiotics and secrete the β-lactamase FTN_1072. Taking advantage of this, we developed an alternative assay to detect cytosolic bacteria based on the cleavage of the FRET (Förster resonance energy transfer) probe CCF4 by the β-lactamase FTN_1072 leading to a loss of FRET activity[31, 32] (Supplementary Fig. 5). Wild-type, *Gbp2*$^{-/-}$ and *Gbp*^{chr3}-deleted BMDMs were preloaded with CCF4-AM, the membrane permeable form of the reporter, and subsequently infected with wild-type *F. novicida*, a FTN_1072-deficient strain (Δ*bla*) or a ΔFPI mutant. No difference between wild-type, *Gbp2*$^{-/-}$ or *Gbp*^{chr3}-deleted BMDMs was observed in terms of FRET activity when infected with wild-type *F. novicida* (Fig. 5b and Supplementary Fig. 5). The ΔFPI and Δ*bla* mutant strains did not produce any significant FRET signals, comparable to uninfected macrophages (Supplementary Fig. 5). Thus we concluded that GBPs did not control AIM2 activation by promoting the escape of *F. novicida* from phagosomes, but that they were active after *F. novicida* reaches the cytosol. This was consistent with the notion that in unprimed cells *F. novicida*-induced *Gbp* mRNA expression was dependent on the *F. novicida* pathogenicity island (FPI) and on phagosomal escape (Fig. 2b) and that cytosolic recognition was required for the interferon-induction (Supplementary Fig. 1a).

GBPs promote cytosolic lysis of *F. novicida*

To identify the mechanism by which GBPs controled AIM2 activation during *F. novicida* infections, we investigated the subcellular localization of GBPs in infected cells. GBPs are known to co-localize with vacuolar pathogens such as *Salmonella typhimurium*, *Mycobacterium bovis* BCG and *Toxoplasma gondii*, consistent with their ability to recruit anti-microbial effector mechanisms to the pathogen and to destabilize PCVs[24, 27, 29]. We observed that both GBP2 and GBP5 were targeted to intracellular *F. novicida* (Fig. 6a). Closer examination of GBP-positive *F. novicida* revealed that GBPs localized to different spots close to or onto the surface of the bacterium. Yet, it was unclear if GBPs targeted the bacterium directly, host membrane remnants (i.e. lysed phagosomes) or another closely associated membrane compartment.

Since the irregular shape of GBP-positive bacteria suggested that they were lysed, we next determined if wild-type and *Gbp*^{chr3}-deleted cells differed in the percentage of lysed intracellular *F. novicida*. The percentage of viable and lysed intracellular bacteria can be quantified based on propidium iodide (PI) staining since intact bacteria remain protected from PI influx (Fig. 6b)[33]. We tested the assay by quantifying lysed bacteria in wild-type BMDMs infected with wild-type *F. novicida* and a *fopA* mutant. A mutation in *fopA* reduces membrane stability of *F. novicida* and results in increased intracellular lysis and hyperactivation of the AIM2 inflammasome[15]. We detected significantly higher amounts of PI^{+} *fopA* bacteria than wild-type *F. novicida*, thus validating our assay (Fig. 6c). We next compared the frequency of lysed bacteria between wild-type and *Gbp*^{chr3}-deleted macrophages. BMDMs from *Gbp*^{chr3}-deleted mice had significantly lower frequencies of lysed (anti- *F. novicida* $^{+}$PI^{+}) bacteria (23% on average) than wild-type cells (40% on average) (Fig. 6c).

The macromolecular inflammasome complex, known as an ASC speck, assembles on genomic DNA that is released from lysed cytosolic *F. novicida*[10]. Immunofluorescence

analysis revealed mostly irregularly shaped *F. novicida* in the vicinity of ASC specks (Fig. 6d). These bacteria released DNA and were often also positive for GBP staining (Fig. 6d, Supplementary Fig. 6). Consistently, the number of ASC speck-containing cells was significantly reduced in *Gbp*-deficient (*Gbp2*$^{-/-}$, *Gbp5*$^{-/-}$, *Gbp*^{chr3}-deleted) BMDMs compared to wild-type cells (Fig. 6e). In conclusion, these findings indicated that GBPs associate with cytosolic *F. novicida* and by a yet undefined mechanism induce the lysis of the bacterium, resulting in DNA release and detection by the cytosolic DNA sensor AIM2 followed by ASC oligomerization.

GBPs control *F. novicida* replication

Inflammasome-induced cell death (pyroptosis) restricts intracellular bacteria by removing their replicative niche and re-exposing them to extracellular immune mechanisms[34]. Cell-autonomous immunity on the other hand relies on cell-intrinsic mechanisms to restrict bacterial growth without a need for killing the host cell[21]. To determine whether GBPs restrict *F. novicida* growth through cell-autonomous or inflammasome-dependent mechanisms, we infected wild-type, *Aim2*$^{-/-}$, *Gbp*^{chr3}-deleted and *Ifnar1*$^{-/-}$ BMDMs with GFP^{+} wild-type *F. novicida* and used flow cytometry to quantify the percentage of infected cells (>2 bacteria per cell, our specific fluorescence detection threshold) among the live cell population (Fig. 7a). We observed a significantly higher percentage of live infected *Aim2*$^{-/-}$, *Gbp*^{chr3}-deleted and *Ifnar1*$^{-/-}$ BMDMs compared with wild-type cells. This suggested that *Ifnar1*- or *Gbp*^{chr3}-deficiency, similarly to *Aim2*-deficiency, resulted in a reduction of inflammasome-mediated host cell killing upon infection.

Cell-autonomous growth restriction is an IFN-induced mechanism, which is, at least partially, independent of inflammasome-mediated cell death[35, 36]. Therefore we next determined if *Gbp*^{chr3}-deleted and *Ifnar1*-deficient BMDMs also had a defect in restricting intracellular bacterial replication. We infected macrophages with GFP^{+}-*F. novicida* and determined the number of bacteria per cell by both automated microscopy in flow (ImageStream™, see Methods section) and microscopy-based enumeration at different timepoints post infection (Fig. 7b, Supplementary Fig. 7a, 7b). Wild-type macrophages efficiently controlled intracellular replication, but *Aim2*$^{-/-}$ BMDMs contained high numbers (30 and more) of intracellular *F. novicida*, which is consistent with a loss of inflammasome mediated killing of host cells. Bacterial loads were even higher in *Gbp*^{chr3}-deleted and *Ifnar1*-deficient BMDMs, with many cells containing up to 100 bacteria. ROS and NO production are potent cell-intrinsic anti-microbial mechanisms that could also be activated in an IFN-dependent manner. GBP7 was shown to recruit subunits of NADPH oxidase to intracellular *L. monocytogenes* and *M. bovis* BCG[24], and the inducible Nitric Oxide synthase (iNOS) can restrict bacterial growth in a cell-intrinsic manner[21]. However, deficiency in these mechanisms using either *Nos2*$^{-/-}$ or *Cybb*$^{-/-}$ BMDMs did not significantly alter bacteriolysis and inflammasome activation upon *F. novicida* infection (Supplementary Fig. 8a, 8b). Overall, these data indicated that GBPs on chromosome 3 participated in growth restriction in two ways: directly by promoting the lysis of intracellular bacteria by a yet unknown mechanism, and indirectly by promoting the inflammasome-mediated killing of host cells thereby removing the intracellular replicative niche of *F. novicida*.

GBPs control *F. novicida* replication *in vivo*

AIM2, ASC and caspase-1 control the replication of *F. novicida in vivo* in mice[9, 10, 37]. Since GBPs are required for inflammasome activation *in vitro*, we investigated whether these proteins also play a physiological role in host defense. Age- and sex-matched wild-type, *Casp1*$^{-/-}$*Casp11*$^{-/-}$, *Gbp2*$^{-/-}$ and *Gbp*^{chr3}-deleted mice were infected subcutaneously with 5×10^3 CFU of wild-type *F. novicida* U112 (Fig. 8a), and the bacterial burden in liver and spleen was determined at 2 days post infection. As published previously[37], *Casp1*$^{-/-}$*Casp11*$^{-/-}$ animals displayed significantly higher bacterial burden in liver and spleen compared to wild-type animals. Similarly *Gbp2*$^{-/-}$ and *Gbp*^{chr3}-deleted mice showed higher bacterial counts (CFU) than wild-type animals, comparably or even higher than *Casp1*$^{-/-}$ *Casp11*$^{-/-}$ animals (Fig. 8a). Consistent with reduced inflammasome activation *in vivo*, we detected significantly reduced concentration of serum IL-18 in *Casp1*$^{-/-}$ *Casp11*$^{-/-}$, *Gbp2*$^{-/-}$ and *Gbp*^{chr3}-deleted mice (Fig. 8b). To further examine the effects of *Gbp*-deficiency *in vivo*, we performed a survival analysis (Fig. 8c). Within 4 days after injection all *Casp1*$^{-/-}$*Casp11*$^{-/-}$, *Gbp2*$^{-/-}$ and *Gbp*^{chr3}-deleted mice died, while most wild-type animals survived until the end of the experiment (day 10). These results confirmed the relevance of our *in vitro* data and demonstrated that GBPs on chromosome 3 were important for inflammasome activation and host defense against *F. novicida in vivo*.

DISCUSSION

Since AIM2 activation during infections with the cytosolic pathogen *F. novicida* infection required IFN signaling, we investigated the role of ISGs in this process. Our results showed that IFN-inducible GTPases GBP2 and GBP5 promote *F. novicida*-mediated AIM2 inflammasome activation, while being dispensable for AIM2 activation upon DNA transfection. GBP family members take part in IFN-induced cell-autonomous immunity and are known to induce the disruption of PCVs of vacuolar bacteria and parasites[23, 27, 29]. However cytosolic localization of *F. novicida* was comparable between wild-type and *Gbp*^{chr3}-deleted cells, indicating that GBPs must be involved later during infection, after the bacteria had entered the cytosol. This notion was consistent with results showing that phagosomal escape is an IFN-independent process[36] and that cytosolic localization of *F. novicida* is a prerequisite for IFN induction[17]. Since AIM2 activation during *F. novicida* and *L. monocytogenes* infection is known to require cytosolic bacteriolysis [12, 15], we determined if GBPs controlled bacteriolysis and replication of *F. novicida* in the cytosol. Significantly less lysed and higher overall numbers of *F. novicida* were found in *Gbp*- and *Ifnar1*-deficient cells than in wild-type cells, indicating that GBPs were required for IFN-mediated cell-autonomous immunity against the pathogen. Furthermore our results demonstrated that besides their known function in destabilizing PCVs, GBPs can also promote bacteriolysis of cytosolic bacteria.

GBPs are also critical for cytosolic LPS recognition and the activation of the caspase-11 inflammasome pathway. In this context they act by promoting the release of vacuolar *S. typhimurium* into the cytosol or by promoting caspase-11 activation during *L. pneumophila* infection[29, 38]. Currently, no model fully explains how GBPs restrict pathogen growth during microbial and protozoan infections and at the same time control inflammasome

signaling. It is however conceivable that the membrane-destabilizing activity of GBPs in combination with their bacteriolytic activity could not only result in the entry of bacteria into the cytosol, but also release microbe-associated molecular patterns (MAMPs, e.g. LPS and DNA) directly. Such a model might explain their impact on both the caspase-11[38] and the AIM2 pathways in response to cytosolic bacteria. Thus bacteriolysis would also release *F. novicida* LPS into the cytosol. However since *F. novicida* LPS is tetra-acylated it does not trigger caspase-11 activation[39]. Conversely, we would expect GBPs to lyse cytosolic *Salmonella* or *Legionella*, resulting in AIM2 activation. But in this case AIM2 activation is most likely masked by a high degree of caspase-11-dependent cell death and cytokine release.

GBP-mediated bacteriolysis could also be expected to release DNA and amplify type-I-IFN production via STING. Notably, what triggers initial STING signaling and *Gbp* induction during *F. novicida* infection is still undefined, but two possibilities exist. One is the direct activation of STING via a secreted bacterial cyclic nucleotide in analogy to *L. monocytogenes* infection[40] and a second is the activation of the DNA sensor cGAS by *F. novicida* DNA and subsequent production of the cyclic dinucleotide cGAMP[41, 42]. Lysis of *F. novicida* within the phagosome followed by translocation of DNA into the cytosol could trigger IFN production[9]. Alternatively, low levels of *F. novicida* extracellular DNA could reach the cytosol by sticking to the surface of the infecting bacteria as suggested during *M. tuberculosis* infection[43]. Finally, low spontaneous bacteriolysis could occur in the host cell cytosol. If DNA indeed triggers initial STING-mediated IFN production, it remains to be shown why it is insufficient to trigger AIM2 activation. Additional experiments are needed to determine the relative DNA binding affinity of cGAS and AIM2 and how their signaling hierarchy is controlled.

Our results have revealed a yet underappreciated close connection between cell-autonomous immunity and innate immune recognition. Preceding attack by GBPs on PCVs or pathogens liberates MAMPs and thus ensures subsequent immune recognition of the pathogen, explaining the role of IFN signaling in the detection of bacterial DNA by AIM2 or LPS from vacuolar bacteria by the caspase-11 pathway[9, 10, 13, 44, 45]. Important questions remain, such as how is GBP targeting regulated and how do GBPs act mechanistically? Ectopic expression of GBP2 or GBP5 did not rescue inflammasome deficiency in *Ifnar1*$^{-/-}$ cells, suggesting that other ISGs are necessary for proper targeting and activity of GBPs[24, 25]. Indeed, IRGMs, a subclass of the immunity-related GTPases (IRGs), can act as guanine-dissociation inhibitors and control both IRG and GBP targeting to pathogen-containing vacuoles, yet the molecular mechanism is still unclear[46, 47, 48, 49]. Additional biochemical studies are necessary to define the mechanism of GBP targeting and action during bacterial infection and how this promotes the exposure of bacterial ligands to cytosolic recognition pathways.

METHODS

Bacterial strains and plasmids

F. novicida U112 and isogenic mutants ΔFPI were published before[10]. When applicable, strains were transformed with pKK219-GFP (Supplementary Table 2). The β-lactamase

mutant (Δ*bla*) was generated by PCR-mediated homologous recombination with a Kanamycin selection casette using the following primers: ForUpstream: GTCGAGTACGCTAATATAAAAATTCTAAAAA, RevUpstream: gcttatcgataccgtcgacctcGGGATTAATGATAAAGTTGTAACTAATATACGC, ForDownstream: gatatcgatcctgcagctatgcCACTTATAAATAAGCGGTACGCCAC, RevDownstream: AAGACGGTGATGTACCATTTGTCTATAG. The kanamycin resistance casette was removed by transforming the obtained mutant with the thermosensitive plasmid pFFlp (kindly provided by Larry Gallagher and Colin Manoil) encoding the Flp recombinase. Following loss of the plasmid, genomic deletion was verified by sequencing.

Mice

Gbp^{chr3}-deleted, *Gbp2*$^{-/-}$, *Gbp5*$^{-/-}$, *Nos2*$^{-/-}$*Cybb*$^{-/-}$, *Casp1*$^{-/-}$*Casp11*$^{-/-}$ (a.k.a caspase-1 knockout), *Asc*$^{-/-}$, *Aim2*$^{-/-}$, *Stat1*$^{-/-}$, *Ifnar1*$^{-/-}$, *Sting*$^{Gt/Gt}$, *Tlr2*$^{-/-}$ and *Myd88*$^{-/-}$ mice have been previously described[3, 10, 23, 27, 29, 44]. Mice were bred in the animal facilities of the University of Basel or at the PBES (Lyon, France).

Animal infection

All animal experiments were approved (license 2535, Kantonales Veterinäramt Basel-Stadt and ENS_2012_061) and performed according to local guidelines (Tierschutz-Verordnung, Basel-Stadt and CECCAPP, Lyon) and the Swiss animal protection law (Tierschutz-Gesetz). Ageand sex-matched animals (8–10 weeks old) were infected subcutaneously with 5×10^3 or 1.5×10^5 CFU of stationary phase wild-type *F. novicida* U112 in 50 µl PBS. Animals were sacrificed at the indicated timepoint post infection. No randomization or blinding was performed.

Cell culture and infections

BMDMs were differentiated in DMEM (Invitrogen) with 10% v/v FCS (Thermo Fisher Scientific), 10% MCSF (L929 cell supernatant), 10 mM HEPES (Invitrogen), and nonessential amino acids (Invitrogen). 1 day before infection, macrophages were seeded into 6-, 24-, or 96-well plates at a density of 1.25×10^6, 2.5×10^5, or 5×10^4 per well. If required macrophages were pre-stimulated with PAM3CSK4, LPS O111:B4 (InvivoGen), mIFN-β or mIFN-γ (eBioscience). For infections with *F. novicida*, bacteria were grown overnight in BHI or TSB at 37 °C with aeration. The bacteria were added to the macrophages at multiplicity of infection (MOI) of 100, or as otherwise indicated. The plates were centrifuged for 15 min at 500 g to ensure comparable adhesion of the bacteria to the cells and placed at 37 °C for 120 min. Next, cells were washed and fresh medium with 10 µg/ml gentamycin (Invitrogen) was added to kill extracellular bacteria and plates were incubated for the desired length of time. Transfection with poly(dA:dT) or poly(dG:dC) was done as described previously[29] or as indicated.

siRNA knockdown

Gene knockdown was done using GenMute (SignaGen laboratories) and siRNA pools (siGenome, Dharmacon). Briefly, wild-type BMDMs were seeded into 24-, or 96-well plates at a density of 1.5×10^5 or 3×10^4 per well. siRNA complexes were prepared at 25 nM siRNA

in GenMute Buffer according to the manufacturer's instructions for forward knockdowns. siRNA complexes were mixed with BMDM medium and added onto the cells. BMDMs were infected with *F. novicida* at an MOI of 100:1 after 22-48 h of knockdown and analyzed for inflammasome activation as outlined below. siRNA pools included: Aim2 (M-044968-01), Casp11 (that is, Casp4) (M-042432-01), Gbp1 (M-040198-01), Gbp2 (M-040199-00), Gbp3 (M-063076-01), Gbp4 (M-047506-01), Gbp5 (M-054703-01), Gbp6 (M-041286-01), Gbp7 (M- 061204-01), Gbp8 (M-059726-01), Gbp9 (M-052281-01), Gbp10 (M-073912-00), Gbp11 (M-079932-00) and NT (non-targeting) pool 2 (D-001206-14).

siRNA screening

Knockdown for the 483 selected genes was performed in triplicates as described above in the 36 central wells of 96 well plates including NT, ASC and Aim2 siRNA on every plates. Macrophages were infected with *F. novicida* at a MOI of 100:1 and following a wash at 1 h post infection, cells were incubated with medium supplemented with propidium iodide at 5 μg/ml. At 6 h post infection, propidium iodide fluorescence was determined on a plate reader (Tecan) and supernatant was collected to dose IL-1β release by ELISA (DuoSet R&D systems). Propidium iodide fluorescence and IL-1β concentration of individual siRNA were normalized to the average value of the full plate set at 100 and to the value of AIM2 siRNA set at 0 using the following calculation: Normalized value $siRNA_X$=(value $siRNA_x$-value $siRNA_{AIM2}$)/(average value siRNA-value $siRNA_{AIM2}$). All the siRNA presenting more than 50% variation in either one of the two parameters have been retested two or three times. Average normalized values are shown.

Ectopic expression of GBP2 and GBP5

mGbp2 and mGbp5 were cloned into the lentiviral plasmid TRIP iziE-SSFV-GFP using the following primers and the indicated restriction enzymes: For_mGBP2_AvrII attacctaggGACATGGCCTCAGAGATCCACATG, Rev_mGBP2_EcoRV aatagataTCAGAGTATAGTGCACTTCCCAGACG, For_mGBP5_AvrII aaatcctagGACATGGCCCCAGAGATTCACATG, Rev_mGBP5_HpaI: atttgttaacttagcttataacacagtcatgatgatgtctac. Lentiviruses production in 293T cells and transduction of primary bone marrow derived macrophages were performed using standard methods. Briefly, IFNAR1-deficient macrophages were transduced after eight days of differentiation by spinoculation (1500 g for 2h at room temperature). Transduced macrophages were infected 48h later. Transduction frequency was determined by flow cytometry based on GFP expression. Specific ectopic expression was checked by qRT-PCR.

Cytokine and LDH release measurement

IL-1β, IL-18 and tumour necrosis factor (TNF) was measured by ELISA (eBioscience). LDH was measured using LDH Cytotoxicity Detection Kit (Clontech). To normalize for spontaneous lysis, the percentage of LDH release was calculated as follows: (LDH infected - LDH uninfected)/(LDH total lysis - LDH uninfected)*100.

Immunoblotting

Blotting was done as described before [29]. Antibodies used were rat anti-mouse caspase-1 antibody (1:1,000; 4B4; Genentech), rabbit anti-IL-1α (1:1,000; ab109555; Abcam), rabbit anti-IL-18 (1:500; 5180R; Biovision), goat anti-mouse IL-1β antibody (1:500; AF-401-NA; R&D Systems) and rabbit anti-GBP2 (1:1,000; 11854-1-AP; Proteintech) and rabbit anti-GBP5 (1:1,000; 13220-1-AP; Proteintech). Cell lysates were probed with monoclonal anti-β-actin antibody (Sigma, AC-15, A1978) at 1:2,000.

Real-time PCR

Primers used for mRNA quantification are described in Supplementary Table 3. Experiments were performed with an iCycler (Bio-Rad) using SYBR green (Applied Biosystems) and standard protocols.

Statistical analysis

Statistical data analysis was done using Prism 5.0a (GraphPad Software, Inc.). To evaluate the differences between two groups (cell death, cytokine release, FACS, CFU and immunofluorescence-based counts) the two-tailed t-test was used. Komogorov-Smirnov test was used to compare the cell distribution as determined by ImageStream™. P values were adjusted for multiple comparisons with the Bonferroni correction approach. Animals experiments were evaluated using Mann-Whitney or log-rank Cox-Mantel test. In figures NS indicates ‘not significant’, P values are explained in figure legends.

Immunofluorescence

Macrophages were seeded on glass coverslips and infected as described above. At the desired time points cells were washed 3x with PBS and fixed with 4% paraformaldehyde for 15 min at 37 °C. Following fixation coverslips were washed and the fixative was quenched with 0.1 M glycine for 10 min at room temperature. Coverslips were stained with primary antibodies at 4 °C for 16 h, washed with PBS, incubated for 1 h with appropriate secondary antibodies at room temperature (1:500, AlexaFluor, Invitrogen), washed with PBS and mounted on glass slides with Vectashield containing 6-diamidino-2-phenylindole (DAPI) (Vector Labs). Antibodies used were chicken anti- *F. novicida* (1:1000, a gift from D. Monack), rat anti-ASC (1:1000, Genentech), rabbit anti-GBP2 and rabbit anti-GBP5 (1:100; 11854-1-AP/13220-1-AP; Proteintech). Coverslips were imaged on a Zeiss LSM700 or a Leica SP8 at 63x magnification and enumeration of vacuolar vs. cytosolic bacteria, total intracellular bacteria or ASS specks was done as described in the figure legends.

Phagosome protection assay

For quantification of cytoplasmic and vacuolar bacteria, macrophages were infected with GFP^+ *F. novicida* as described above. At the desired time point, cells were washed with KHM buffer (110 mM potassium acetate, 20 mM HEPES, 2 mM MgCl2, pH 7.3) and incubated for 1 min in KHM buffer with 50 μg/ml digitonin (Sigma). Cells were immediately washed 3 times with KHM buffer and then stained for 12 min with anti-*F. novicida* antibodies coupled to TexasRed in KHM buffer with 2% BSA. Cells were washed

with PBS, fixed and analyzed by microscopy. Controls were included in every assay as described before [29].

Intracellular viability measurements

For measuring intracellular lysis of *F. novicida*, we adapted a PI staining method published previously[33]. Infected BMDMs were incubated for 12 min at 37°C with Alexa Fluor™ 488-conjugated mouse anti-*F. novicida* antibodies and 2.6 μM PI (Sigma) in KHM buffer (see above) to label accessible cytosolic bacteria and compromised bacteria, respectively, in permeabilized cells. Cells were fixed and imaged as described above.

CCF4 measurements

Quantification of vacuolar escape using the β-lactamase-CCF4 assay (Life technologies) was performed following manufacturer's instructions. Briefly, macrophages seeded onto non-treated plates were infected as previously described for 1 h, washed and incubated in CCF4 for 1 hour at room temperature in the presence of 2.5 mM probenicid (Sigma). Propidium iodide negative cells were considered for the quantification of cells containing cytosolic *F. novicida* using excitation at 405 nm and detection at 450 nm (cleaved CCF4) or 510 nm (intact CCF4).

Flow cytometry

For assessment of bacterial replication by flow cytometry, macrophages seeded onto non treated plates were infected as described above with GFP-expressing *F. novicida* strains. At 8 h post infection, cells were lifted with trypsin and immediately analyzed by Flow cytometry on a Canto 2 cytometer (BD biosciences). Dead cells were excluded based on staining with propidium iodide.

ImageStream™ flow cytometry

Macrophages infected with GFP expressing bacteria were fixed in PFA 4% and analyzed on ImageStream X mark II (Amnis, EMD-Millipore) using the Inspire software with the Extended depth of field (EDF) function activated to increase the spot counts accuracy. Images of single cells were analyzed with the Ideas Software (Amnis, EMD-Millipore) using the following steps (each step being validated by visualization of at least 20 single cells). Doublets and debris were excluded on morphological parameters (Aspect Ratio and Area in the brightfield channel). Defocused images were eliminated thanks to the Gradient RMS function on the brightfield function. Spot counts and definition of the mean fluorescence of single bacterium: specific GFP fluorescence signal was defined by applying a mask combining an intensity threshold and a spot to cell background ratio (peak) function. Automatic spot count was performed using the above mask. Cells containing a single spot (either a single bacterium or a tight cluster of several bacteria) were gated. The area of the specific signal was analyzed in single cells on the gated population. To exclude bacterial cluster and quantify the fluorescence of single bacterium, the mean fluorescence intensity was calculated on GFP-positive signal covering an area of $1 \pm 0.5\ \mu m^2$ in 1599 cells.

The number of bacteria in single cells determined by the automatic spot count function or calculated based on the fluorescence of single bacterium was identical for cells containing

less than 7 bacteria (R^2>0.99). For higher intracellular burden, the spot count function largely underestimated the number of bacteria per cell due to the difficulty to discriminate bacterial cluster. We thus relied on the specific fluorescence of the bacteria within the cells as defined by the above mask and the calculated fluorescence value of single intracellular bacterium to quantify the number of bacteria per cell. The mask was applied to at least 10'000 images of single cell per sample in order to extract the specific fluorescence of the intracellular bacteria in single cells.

Supplementary Material

Refer to Web version on PubMed Central for supplementary material.

ACKNOWLEDGMENTS

We thank N. Gekara, M. Roth, S. Hofer, D. Monack, N. Kayagaki and V. Dixit for reagents, O. Allatif for statistical analysis and the Biozentrum Imaging and FACS Core Facilities for technical assistance. We acknowledge the contribution of the PBES and the flow cytometry platform of SFR Biosciences Gerland-Lyon Sud. This work was supported by an SNSF Professorship PP00P3_139120/1 and a University of Basel project grant ID2153162 to P.B., by an ERC starting grant 311542 to T.H. and a fellowship from the 'Déléguation Générale de l'Armement '(DGA) to M.R..

REFERENCES

1. Paludan SR, Bowie AG. Immune sensing of DNA. Immunity. 2013; 38:870–880. [PubMed: 23706668]
2. Ishikawa H, Ma Z, Barber GN. STING regulates intracellular DNA-mediated, type I interferon-dependent innate immunity. Nature. 2009; 461:788–792. [PubMed: 19776740]
3. Sauer JD, et al. The N-ethyl-N-nitrosourea-induced Goldenticket mouse mutant reveals an essential function of Sting in the in vivo interferon response to Listeria monocytogenes and cyclic dinucleotides. Infect Immun. 2011; 79:688–694. [PubMed: 21098106]
4. Hornung V, et al. AIM2 recognizes cytosolic dsDNA and forms a caspase-1-activating inflammasome with ASC. Nature. 2009; 458:514–518. [PubMed: 19158675]
5. Fernandes-Alnemri T, Yu JW, Datta P, Wu J, Alnemri ES. AIM2 activates the inflammasome and cell death in response to cytoplasmic DNA. Nature. 2009; 458:509–513. [PubMed: 19158676]
6. Roberts TL, et al. HIN-200 proteins regulate caspase activation in response to foreign cytoplasmic DNA. Science. 2009; 323:1057–1060. [PubMed: 19131592]
7. Burckstummer T, et al. An orthogonal proteomic-genomic screen identifies AIM2 as a cytoplasmic DNA sensor for the inflammasome. Nat Immunol. 2009; 10:266–272. [PubMed: 19158679]
8. Ge J, Gong YN, Xu Y, Shao F. Preventing bacterial DNA release and absent in melanoma 2 inflammasome activation by a Legionella effector functioning in membrane trafficking. Proceedings of the National Academy of Sciences of the United States of America. 2012; 109:6193–6198. [PubMed: 22474394]
9. Fernandes-Alnemri T, et al. The AIM2 inflammasome is critical for innate immunity to Francisella tularensis. Nature immunology. 2010; 11:385–393. [PubMed: 20351693]
10. Jones JW, et al. Absent in melanoma 2 is required for innate immune recognition of Francisella tularensis. Proceedings of the National Academy of Sciences of the United States of America. 2010; 107:9771–9776. [PubMed: 20457908]
11. Kim S, et al. Listeria monocytogenes is sensed by the NLRP3 and AIM2 inflammasome. European journal of immunology. 2010; 40:1545–1551. [PubMed: 20333626]
12. Sauer JD, et al. Listeria monocytogenes triggers AIM2-mediated pyroptosis upon infrequent bacteriolysis in the macrophage cytosol. Cell host & microbe. 2010; 7:412–419. [PubMed: 20417169]

13. Rathinam VA, et al. The AIM2 inflammasome is essential for host defense against cytosolic bacteria and DNA viruses. Nature immunology. 2010; 11:395–402. [PubMed: 20351692]
14. Briken V, Ahlbrand SE, Shah S. Mycobacterium tuberculosis and the host cell inflammasome: a complex relationship. frontiers in cellular and infection microbiology. 2013; 3:62. [PubMed: 24130966]
15. Peng K, Broz P, Jones J, Joubert LM, Monack D. Elevated AIM2-mediated pyroptosis triggered by hypercytotoxic Francisella mutant strains is attributed to increased intracellular bacteriolysis. Cellular microbiology. 2011; 13:1586–1600. [PubMed: 21883803]
16. Muruve DA, et al. The inflammasome recognizes cytosolic microbial and host DNA and triggers an innate immune response. Nature. 2008; 452:103–107. [PubMed: 18288107]
17. Henry T, Brotcke A, Weiss DS, Thompson LJ, Monack DM. Type I interferon signaling is required for activation of the inflammasome during Francisella infection. J Exp Med. 2007; 204:987–994. [PubMed: 17452523]
18. Cole LE, et al. Macrophage proinflammatory response to Francisella tularensis live vaccine strain requires coordination of multiple signaling pathways. J Immunol. 2008; 180:6885–6891. [PubMed: 18453609]
19. Cole LE, et al. Toll-like receptor 2-mediated signaling requirements for Francisella tularensis live vaccine strain infection of murine macrophages. Infect Immun. 2007; 75:4127–4137. [PubMed: 17517865]
20. Jones JW, Broz P, Monack DM. Innate immune recognition of francisella tularensis: activation of type-I interferons and the inflammasome. Front Microbiol. 2011; 2:16. [PubMed: 21687410]
21. Kim BH, Shenoy AR, Kumar P, Bradfield CJ, MacMicking JD. IFN-inducible GTPases in host cell defense. Cell host & microbe. 2012; 12:432–444. [PubMed: 23084913]
22. Howard JC, Hunn JP, Steinfeldt T. The IRG protein-based resistance mechanism in mice and its relation to virulence in Toxoplasma gondii. Current opinion in microbiology. 2011; 14:414–421. [PubMed: 21783405]
23. Yamamoto M, et al. A cluster of interferon-gamma-inducible p65 GTPases plays a critical role in host defense against Toxoplasma gondii. Immunity. 2012; 37:302–313. [PubMed: 22795875]
24. Kim BH, et al. A family of IFN-gamma-inducible 65-kD GTPases protects against bacterial infection. Science. 2011; 332:717–721. [PubMed: 21551061]
25. Degrandi D, et al. Extensive characterization of IFN-induced GTPases mGBP1 to mGBP10 involved in host defense. J Immunol. 2007; 179:7729–7740. [PubMed: 18025219]
26. Kresse A, et al. Analyses of murine GBP homology clusters based on in silico, in vitro and in vivo studies. BMC Genomics. 2008; 9:158. [PubMed: 18402675]
27. Degrandi D, et al. Murine guanylate binding protein 2 (mGBP2) controls Toxoplasma gondii replication. Proc Natl Acad Sci U S A. 2013; 110:294–299. [PubMed: 23248289]
28. Kravets E, et al. The GTPase activity of murine guanylate-binding protein 2 (mGBP2) controls the intracellular localization and recruitment to the parasitophorous vacuole of Toxoplasma gondii. J Biol Chem. 2012; 287:27452–27466. [PubMed: 22730319]
29. Meunier E, et al. Caspase-11 activation requires lysis of pathogen-containing vacuoles by IFN-induced GTPases. Nature. 2014; 509:366–370. [PubMed: 24739961]
30. Checroun C, Wehrly TD, Fischer ER, Hayes SF, Celli J. Autophagy-mediated reentry of Francisella tularensis into the endocytic compartment after cytoplasmic replication. Proc Natl Acad Sci U S A. 2006; 103:14578–14583. [PubMed: 16983090]
31. Nothelfer K, Dias Rodrigues C, Bobard A, Phalipon A, Enninga J. Monitoring Shigella flexneri vacuolar escape by flow cytometry. Virulence. 2011; 2:54–57. [PubMed: 21317555]
32. Juruj C, et al. caspase-1 activity affects AIM2 speck formation/stability through a negative feedback loop. frontiers in cellular and infection microbiology. 2013:1–11. [PubMed: 23355975]
33. Chong A, et al. Cytosolic clearance of replication-deficient mutants reveals Francisella tularensis interactions with the autophagic pathway. Autophagy. 2012; 8:1342–1356. [PubMed: 22863802]
34. Miao EA, et al. Caspase-1-induced pyroptosis is an innate immune effector mechanism against intracellular bacteria. Nature immunology. 2010; 11:1136–1142. [PubMed: 21057511]

35. Zhou H, et al. Genome-wide RNAi screen in IFN-gamma-treated human macrophages identifies genes mediating resistance to the intracellular pathogen Francisella tularensis. PLoS One. 2012; 7:e31752. [PubMed: 22359626]
36. Edwards JA, Rockx-Brouwer D, Nair V, Celli J. Restricted cytosolic growth of Francisella tularensis subsp. tularensis by IFN-{gamma} activation of macrophages. Microbiology. 2009
37. Mariathasan S, Weiss DS, Dixit VM, Monack DM. Innate immunity against Francisella tularensis is dependent on the ASC/caspase-1 axis. J Exp Med. 2005; 202:1043–1049. [PubMed: 16230474]
38. Pilla DM, et al. Guanylate binding proteins promote caspase-11-dependent pyroptosis in response to cytoplasmic LPS. Proceedings of the National Academy of Sciences of the United States of America. 2014; 111:6046–6051. [PubMed: 24715728]
39. Hagar JA, Powell DA, Aachoui Y, Ernst RK, Miao EA. Cytoplasmic LPS activates caspase-11: implications in TLR4-independent endotoxic shock. Science. 2013; 341:1250–1253. [PubMed: 24031018]
40. Woodward JJ, Iavarone AT, Portnoy DA. c-di-AMP secreted by intracellular Listeria monocytogenes activates a host type I interferon response. Science. 2010; 328:1703–1705. [PubMed: 20508090]
41. Sun L, Wu J, Du F, Chen X, Chen ZJ. Cyclic GMP-AMP synthase is a cytosolic DNA sensor that activates the type I interferon pathway. Science. 2013; 339:786–791. [PubMed: 23258413]
42. Li XD, et al. Pivotal roles of cGAS-cGAMP signaling in antiviral defense and immune adjuvant effects. Science. 2013; 341:1390–1394. [PubMed: 23989956]
43. Manzanillo PS, Shiloh MU, Portnoy DA, Cox JS. Mycobacterium tuberculosis activates the DNA-dependent cytosolic surveillance pathway within macrophages. Cell Host Microbe. 2012; 11:469–480. [PubMed: 22607800]
44. Broz P, et al. Caspase-11 increases susceptibility to Salmonella infection in the absence of caspase-1. Nature. 2012; 490:288–291. [PubMed: 22895188]
45. Rathinam VA, et al. TRIF licenses caspase-11-dependent NLRP3 inflammasome activation by gram-negative bacteria. Cell. 2012; 150:606–619. [PubMed: 22819539]
46. Martens S, et al. Disruption of Toxoplasma gondii parasitophorous vacuoles by the mouse p47-resistance GTPases. PLoS Pathog. 2005; 1:e24. [PubMed: 16304607]
47. Howard JC, Hunn JP, Steinfeldt T. The IRG protein-based resistance mechanism in mice and its relation to virulence in Toxoplasma gondii. Curr Opin Microbiol. 2011; 14:414–421. [PubMed: 21783405]
48. Bekpen C, et al. The interferon-inducible p47 (IRG) GTPases in vertebrates: loss of the cell autonomous resistance mechanism in the human lineage. Genome biology. 2005; 6:R92. [PubMed: 16277747]
49. Haldar AK, et al. IRG and GBP host resistance factors target aberrant, “non-self” vacuoles characterized by the missing of “self” IRGM proteins. PLoS pathogens. 2013; 9:e1003414. [PubMed: 23785284]

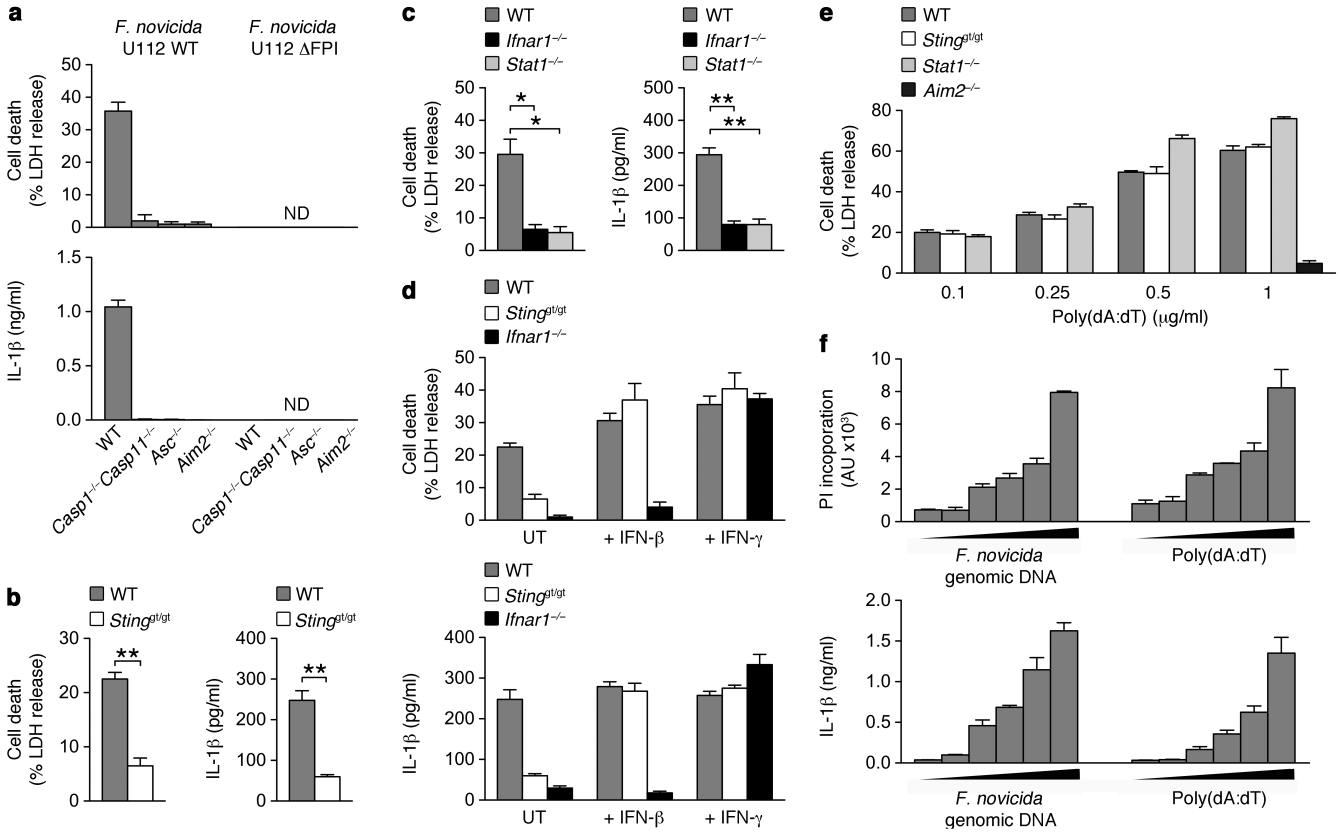

Figure 1.

Interferon-stimulated genes are required for AIM2 activation during *F. novicida* infection. (**a**–**c**) LDH and IL-1β release from unprimed wild-type (WT), *Casp1*$^{-/-}$*Casp11*$^{-/-}$, *Asc*$^{-/-}$, *Aim2*$^{-/-}$, *Sting*$^{Gt/Gt}$, *Ifnar1*$^{-/-}$ or *Stat-1*$^{-/-}$ bone-marrow derived macrophages (BMDMs) infected for 8 h with WT *F. novicida* U112 (**a-c**) or a ΔFPI mutant (**a**). ND, not detectable. (**d**) LDH and IL-1β release from untreated (UT), IFN-β- or IFN-γ-primed wild-type, *Sting*$^{Gt/Gt}$ and *Ifnar1*$^{-/-}$ BMDMs infected for 8 h with WT *F. novicida* U112. Genotypes as indicated. (**e**) LDH release from WT, *Sting*$^{Gt/Gt}$, *Stat1*$^{-/-}$ and *Aim2*$^{-/-}$ BMDMs transfected with indicated amounts of poly(dA:dT). (**f**) Cell death (measured by propidium iodide (PI) incorporation) and IL-1β release from PAM3CSK4-primed WT BMDMs transfected for 1 h with 0, 20, 100, 250, 500 and 1000 ng/ml of purified *F. novicida* genomic DNA or poly(dA:dT). Graphs show mean and s.d. of quadruplicate wells and data are representative of two (**b**, **d**, **f**) and three (**a**, **c**, **e**) independent experiments. *, p<0.001; **, p<0.001 (two-tailed unpaired t-test).

Europe PMC Funders Author Manuscripts

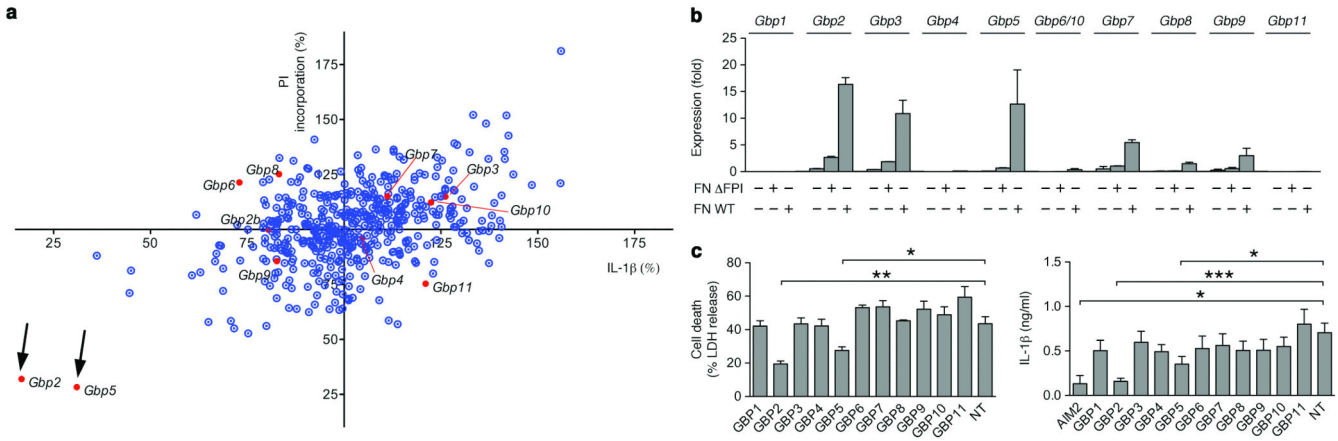

Figure 2.

RNA interference screening identifies members of the GBP family as important AIM2 activators. (**a**) Summary of siRNA screening results in wild-type (WT) BMDMs showing percentage of propidium iodide incorporation and IL-1β release normalized to the average values of all siRNA (100%) and to AIM2 siRNA values (0%). GBP protein family members are highlighted in red. GBP2 and GBP5 are indicated by black arrows. (**b**) Relative mRNA expression of different murine *Gbp* genes in wild-type BMDMs left uninfected or infected with *F. novicida* (FN) WT U112 or an ΔFPI mutant for 8 h. (**c**) LDH and IL-1β release from unprimed WT BMDMs infected for 8 h with WT *F. novicida* U112. BMDMs were treated with the indicated siRNA for 48 h before infection. Bar graphs show mean and s.d. of quadruplicate wells and data are representative of one (**a**), two (**b**) and three (**c,** LDH) independent experiments or pooled data from 6 independent experiments (**c,** IL-1β). *, $p<0.05$; **, $p<0.01$; ***, $p<0.001$ (two-tailed unpaired t-test).

Europe PMC Funders Author Manuscripts

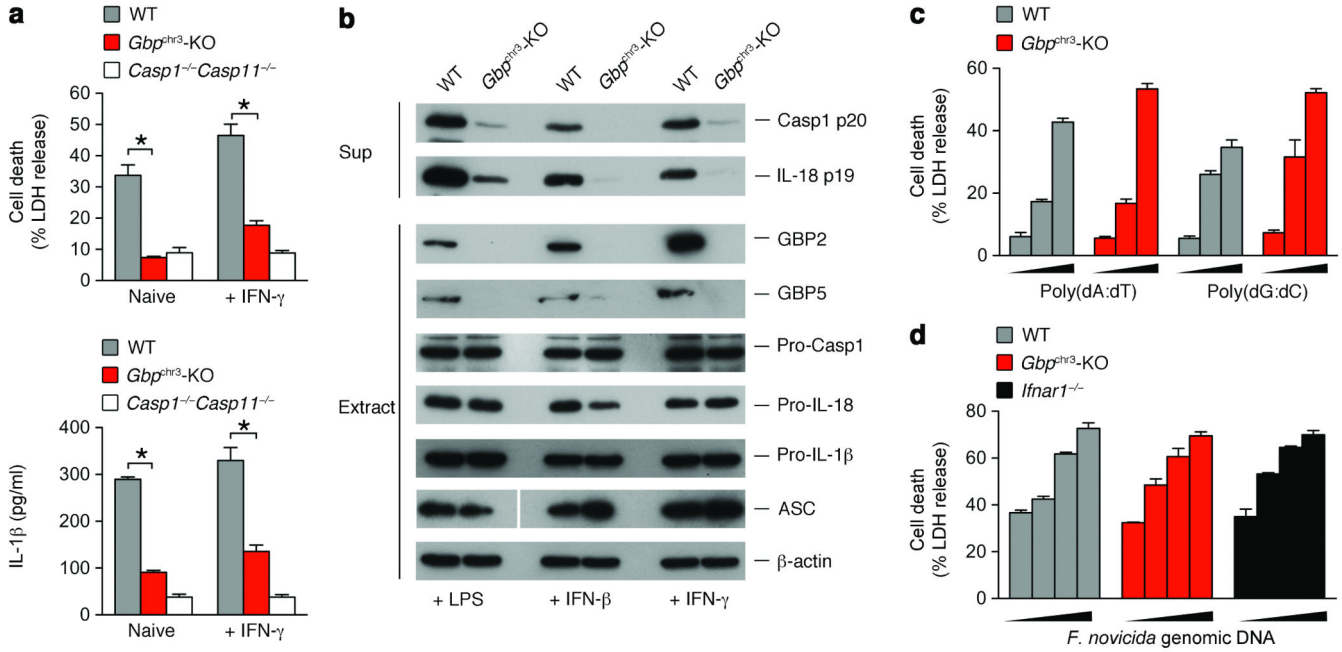

Figure 3.

Macrophages from *Gbp*^{chr3}-deleted mice are deficient for AIM2 activation in response to *F. novicida*. (**a**) LDH and IL-1β release from naive or IFN-γ-primed wild-type (WT), *Gbp*^{chr3}-deleted (*Gbp*^{chr3}-KO) and *Casp1*$^{-/-}$*Casp11*$^{-/-}$ BMDMs infected for 8 h with WT *F. novicida* U112. (**b**) Immunoblot analysis of cleaved caspase-1 p20 and IL-18 p19 in the culture supernatants (Sup) and procaspase-1, pro-IL-18, pro-IL-1β, ASC, GBP2, GBP5 and β-actin in the cell extracts (Extract) of primed WT and *Gbp*^{chr3}-deleted BMDMs infected for 8 h with WT *F. novicida* U112. (**c**) LDH release from WT and *Gbp*^{chr3}-KO BMDMs transfected with 0.25, 0.5 and 1 μg/ml of poly(dA:dT) or poly(dG:dC) for 8 h. (**d**) LDH release from WT, *Gbp*^{chr3}-KO and *Ifnar1*$^{-/-}$ BMDMs transfected with 0.1, 0.25, 0.5 and 1 μg/ml of *F. novicida* genomic DNA for 8 h. Graphs show mean and s.d. of quadruplicate wells and data are representative of two (**d**), three (**b, c**) and six (**a**) independent experiments. *, p<0.001 (two-tailed unpaired t-test).

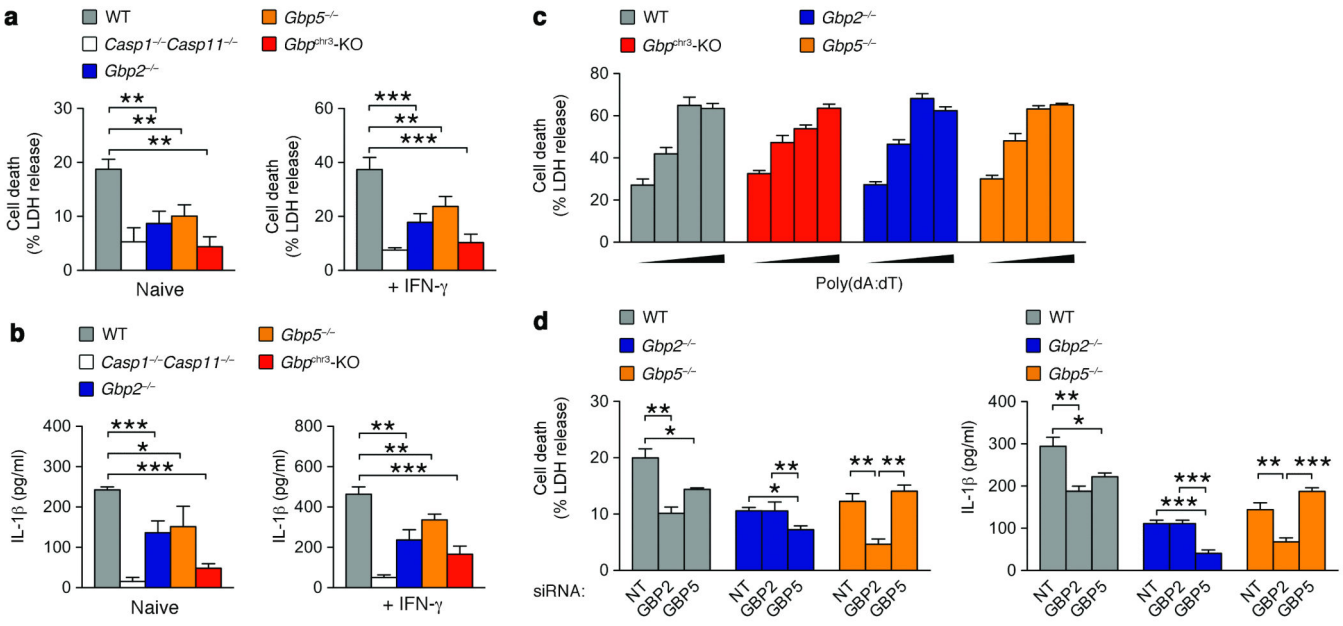

Figure 4.

GBP2 and GBP5 independently control AIM2 activation during *F. novicida* infection. (**a**–**b**) LDH and IL-1β release from naive or IFN-γ-primed wild-type (WT), *Casp1*$^{-/-}$*Casp11*$^{-/-}$, *Gbp2*$^{-/-}$, *Gbp5*$^{-/-}$ and *Gbp*^{chr3}-deleted (*Gbp*^{chr3}-KO) BMDMs infected for 6 h with WT *F. novicida* U112. (**c**) LDH release from naive WT, *Gbp*^{chr3}-deleted, *Gbp2*$^{-/-}$ and *Gbp5*$^{-/-}$ BMDMs transfected with 0.1, 0.25, 0.5 and 1 μg/ml of poly(dA:dT). (**d**) LDH and IL-1β release from naive WT, *Gbp2*$^{-/-}$ and *Gbp5*$^{-/-}$ BMDMs treated with Non-Targeting (NT), GBP2- or GBP5-specific siRNA for 22 h and infected for 8 h with WT *F. novicida* U112. Graphs show mean and s.d. of quadruplicate wells and data are representative of two (**d**), three (**c**) and four (**a, b**) independent experiments. *, p<0.05; **, p<0.01; ***, p<0.001 (two-tailed unpaired t-test).

Europe PMC Funders Author Manuscripts

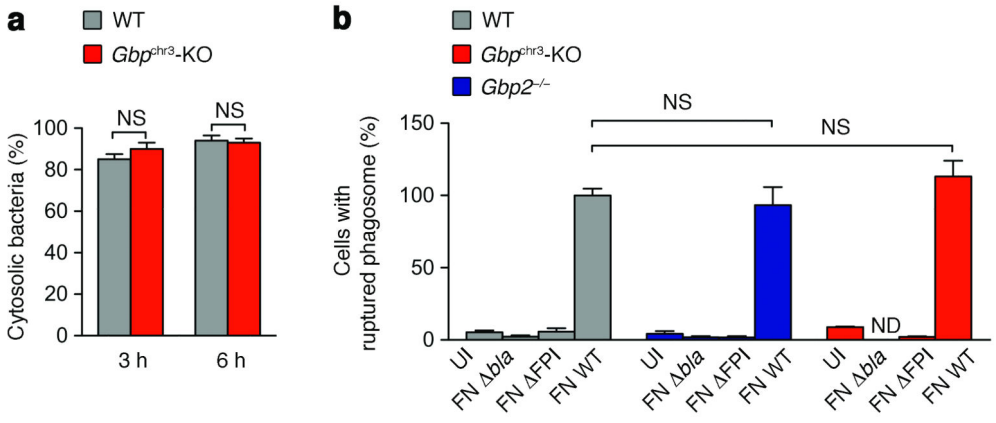

Figure 5.

Phagosomal escape of *F. novicida* is GBP-independent. (**a**) Percentage of cytosolic wild-type (WT) *F. novicida* U112 among total bacteria at 3 h and 6 h post-infection in WT and *Gbp*^{chr3}-deleted BMDMs as determined by phagosome protection assay. (**b**) Percentage of cells with ruptured phagosomes among total cells determined using the β-lactamase-cleavable FRET-probe CCF4 from WT, *Gbp2*$^{-/-}$ and *Gbp*^{chr3}-deleted BMDMs left uninfected (UI) or infected with WT *F. novicida* U112, a β-lactamase-deficient mutant (Δbla) or a ΔFPI mutant at 16 h post infection. Graph shows pooled data from 4 independent experiments with 300 bacteria counted in each (**a**) or pooled data from three independent experiments with 3 × 150,000 cells counted in each (**b**). NS, not significant (two-tailed unpaired t-test).

Europe PMC Funders Author Manuscripts

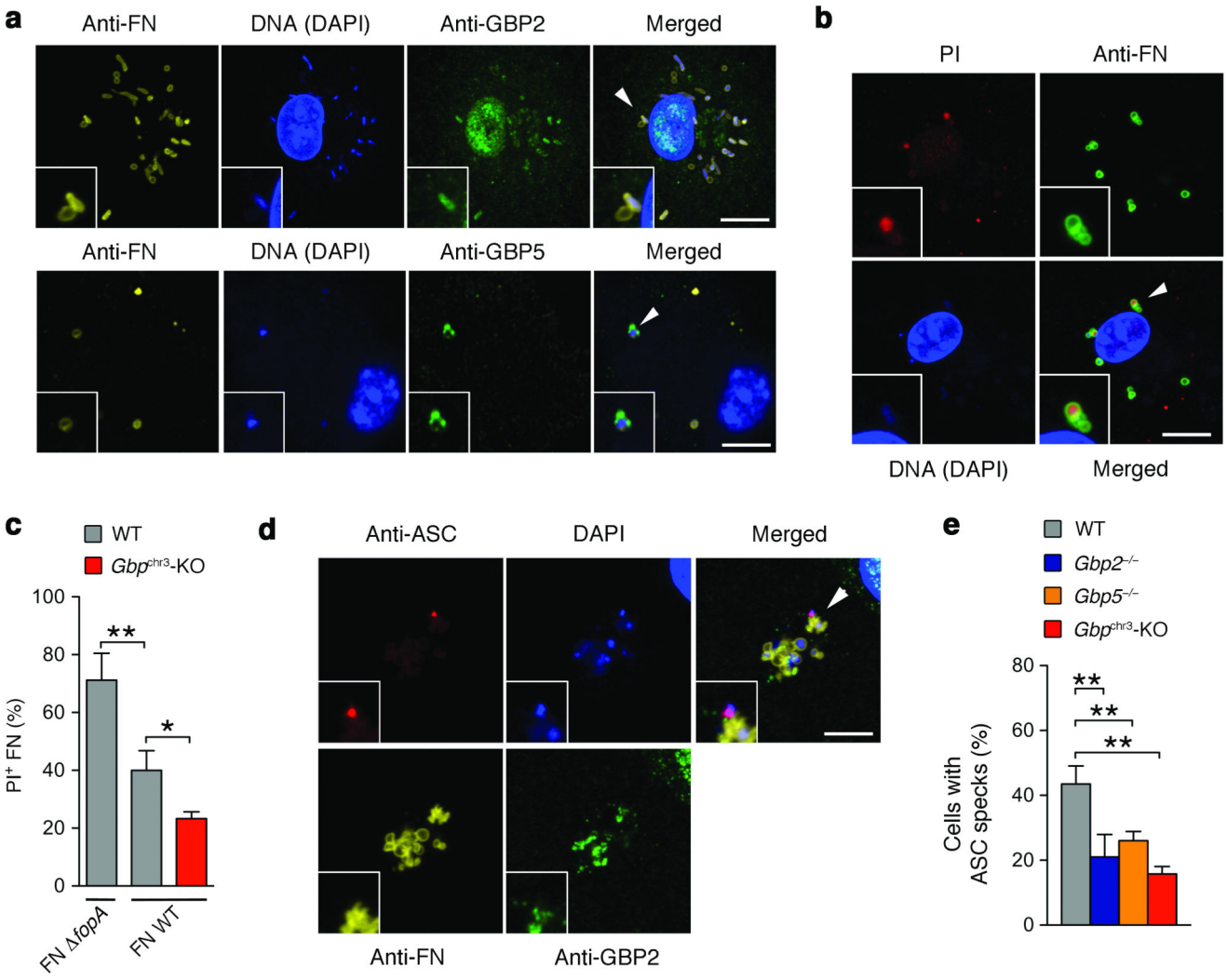

Figure 6.

GBPs promote AIM2 activation by inducing bacteriolysis. (**a**) Immunostaining for GBP2, GBP5 and *F. novicida* (anti-FN) in IFN-γ-primed wild-type (WT) BMDMs infected for 8 h with WT *F. novicida*. (**b**) Imaging of lysed (propidium iodide^{+} *F. novicida*) in IFN-γ-primed WT BMDMs infected for 8 h with WT *F. novicida*. (**c**) Quantification of lysed (propidium iodide^{+} *F. novicida*) in IFN-γ-primed WT and *Gbp*^{chr3}-deleted (*Gbp*^{chr3}-KO) BMDMs infected for 8 h with WT or Δ*fopA F. novicida*. (**d**) Immunostaining for ASC, GBP2 and *Francisella* IFN-γ-primed WT BMDMs infected for 8 h with WT *F. novicida*. (**e**) Quantification of ASC speck formation in IFN-γ-primed WT, *Gbp2*$^{-/-}$, *Gbp5*$^{-/-}$ and *Gbp*^{chr3}-KO BMDMs infected for 8 h with WT *F. novicida*. Graphs in (**c, e**) shows pooled data from 3 independent experiments with 300 bacteria (**c**) or cells (**e**) counted in each. Images (**a, b, d**) are representative of three independent experiments. Scale bars: 10 μm. *, $p<0.05$; **, $p<0.01$ (two-tailed unpaired t-test).

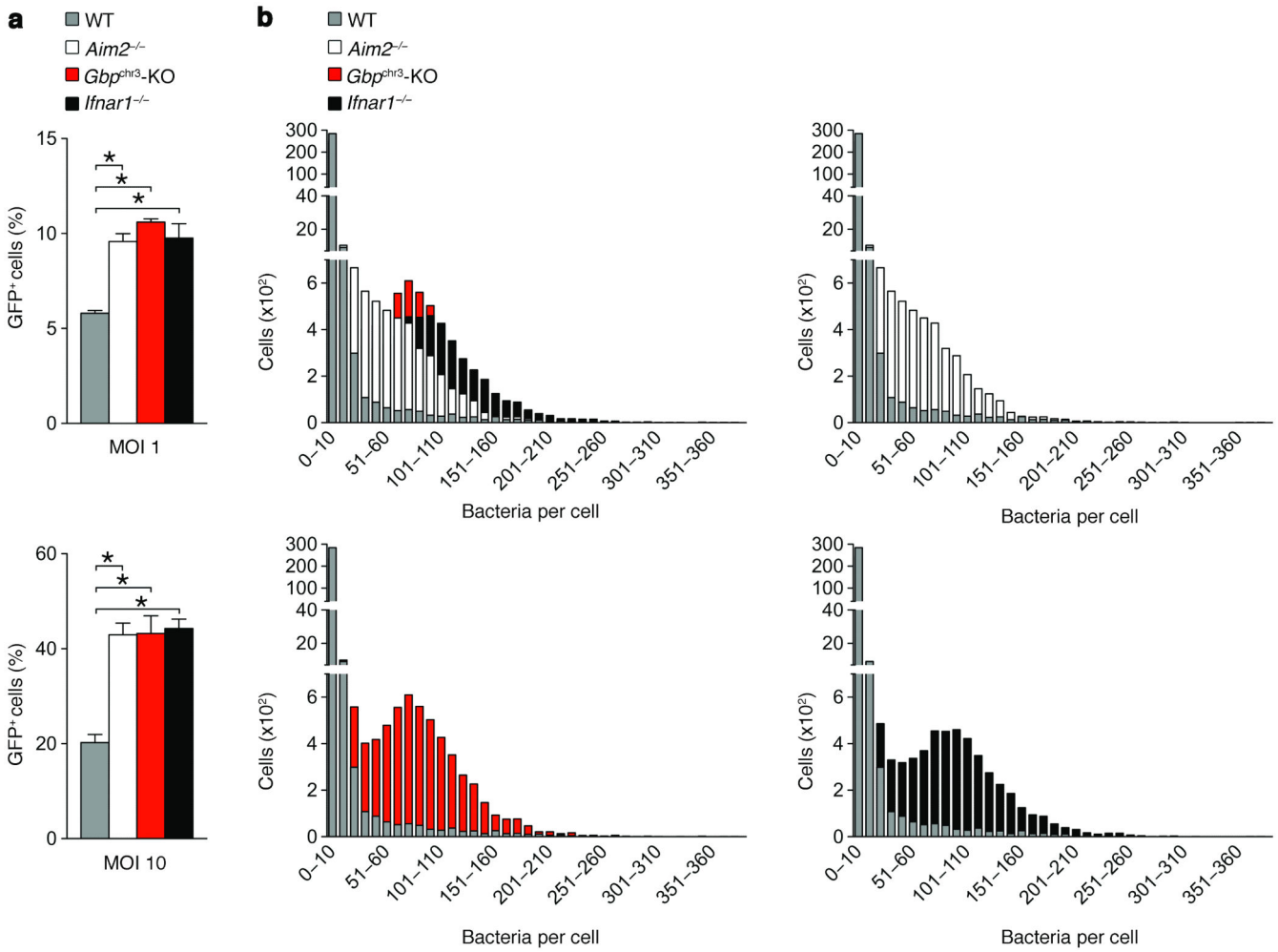

Figure 7.

GBPs restrict intracellular *F. novicida* replication. (**a**) Flow cytometry-based quantification of infected cells (GFP$^+$) among live wild-type (WT), *Aim2*$^{-/-}$, *Gbp*^{chr3}-deleted (*Gbp*^{chr3}-KO) and *Ifnar1*$^{-/-}$ BMDMs infected with GFP$^+$-WT *F. novicida* at an MOI 1 and 10 for 12 h. *, p<0.001 (two-tailed unpaired t-test). Graphs show mean and s.d. of triplicate wells and are representative of three independent experiments. (**b**) Quantification of bacterial loads in single cells by high-resolution microscopy in flow. WT, *Aim2*$^{-/-}$, *Gbp*^{chr3}-KO and *Ifnar1*$^{-/-}$ BMDMs were infected with GFP$^+$ WT *F. novicida* at an MOI of 10 for 12 h, fixed and analyzed by ImageStream™ flow cytometry. Graphs show a comparison of all 4 genotypes (top left panel) or WT cells in comparison to the 3 individual gene-deficient BMDMs. Each bar corresponds to the number of cells with the indicated numbers of bacteria per cell grouped by increments of 10. Pooled data from 3 independent experiments are shown. P vales: WT vs. *Aim2*$^{-/-}$ p<0.0001, WT vs. *Gbp*^{chr3}-KO p<0.0001 and WT vs. *Ifnar1*$^{-/-}$ p<0.0001 (Kolmogorov-Smirnov test with Bonferroni correction).

Europe PMC Funders Author Manuscripts

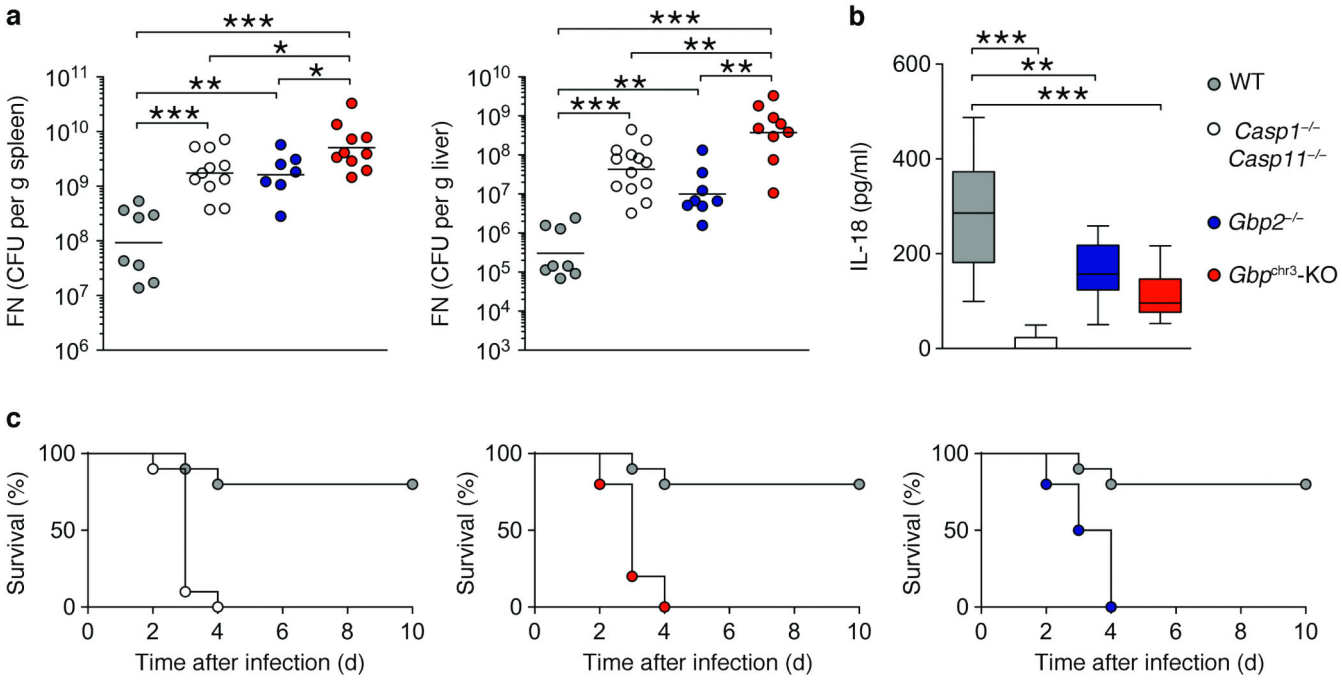

Figure 8.

GBPs control host defense against *F. novicida* (FN) *in vivo*. (**a**) Bacterial burden measured by CFU per g tissue in liver and spleen at day 2 post-infection from wild-type (WT), *Casp1*$^{-/-}$*Casp11*$^{-/-}$, *Gbp2*$^{-/-}$ and *Gbp*^{chr3}-deleted (*Gbp*^{chr3}-KO) mice infected subcutaneously with 5×10^3 WT *F. novicida*. Graphs depict data from 8, 10, 7 and 10 mice (spleen), or 8, 13, 8, and 9 mice (liver) and are representative of two independent experiments. *, p<0.05; **, p<0.01; ***, p<0.001 (Mann-Whitney test). (**b**) Serum IL-18 in WT, *Casp1*$^{-/-}$*Casp11*$^{-/-}$, *Gbp2*$^{-/-}$ and *Gbp*^{chr3}-KO mice infected subcutaneously with 1.5 × 10^5 WT *F. novicida* for 16 h. Data were pooled from 2 individual experiments with a total of 12 (WT), 11 (*Casp1*$^{-/-}$*Casp11*$^{-/-}$), 12 (*Gbp2*$^{-/-}$) and 14 (*Gbp*^{chr3}-KO) mice and are shown as box with means and whiskers (10-90 percentile). **, p<0.01; ***, p<0.001 (Mann-Whitney test). **c**, Survival analysis of WT, *Casp1*$^{-/-}$*Casp11*$^{-/-}$, *Gbp2*$^{-/-}$ and *Gbp*^{chr3}-KO mice infected subcutaneously with 5 × 10^3 WT *F. novicida*. Graphs show from 10 mice per genotype and are representative of two independent experiments. P values: WT vs. *Casp1*$^{-/-}$*Casp11*$^{-/-}$ p<0.0001, wild-type vs. *Gbp*^{chr3}-KO p<0.0001 and wild-type vs. *Gbp2*$^{-/-}$ p=0.0005. Log-rank (Mantel-Cox) test.